LDMA-NOMA beamforming in near-field communication systems

Chenguang Rao, Zhiguo Ding, *Fellow, IEEE*, Kanapathippillai Cumanan, *Senior Member, IEEE* and Xuchu Dai

***Abstract*—In this paper, a novel LDMA-NOMA hybrid beamforming scheme is proposed for near-field communication systems, which improves the performance of both location-division multiple access (LDMA) and non-orthogonal multiple access (NOMA), simultaneously. The key innovation of the proposed scheme is the flexible utilization of user resolution information: LDMA is applied to users with better resolution, while NOMA is used for those users with poor resolution. For each NOMA user, the most suitable beam will be selected by optimizing the system performance and beam efficiency. A unique feature of our scheme is its effectiveness even under limited beam resources. The performance of the scheme is analyzed and the closed-form results are obtained. Simulation results validate the theoretical results and demonstrate superior performance compared to that of the conventional schemes.**

***Index Terms*—Near-field communication, uniform planar array, multiple-input multiple-output (MIMO), location-division multiple access (LDMA), non-orthogonal multiple access (NOMA).**

I. Introduction

In recent decades, wireless communication technologies have advanced rapidly. From the first generation (1G) to the fifth generation (5G) and beyond, the requirements of communication systems have evolved from simple analog audio signal transmission to supporting diverse high-speed, low-latency multimedia services, which highly demands efficient and reliable wireless communication systems [1], [2]. Therefore, designing more efficient, stable, and reliable communication systems to meet the ever-growing demand with limited resources has become a challenging task for the relevant research communities. Among the many technologies, multiple-input multiple-output (MIMO) and extremely large-scale antenna arrays (ELAAs) have emerged as key technologies for next-generation communication systems, which can provide higher spectral and energy efficiencies as well as massive connectivity [3]–[6]. However, as the number of antenna arrays increases, their impact on the physical model becomes non-negligible. Specifically, the radiation region of an antenna array can be divided into the near-field and far-field regions [7], [8]. In the far-field region, electromagnetic waves can be approximated as plane waves, while within the near-field region, they must be considered as spherical waves. The range of the near-field region depends on the number of elements in the antenna array, the spacing between elements, and the frequency of the electromagnetic waves. In the communication system with a small-scale antenna array, the range of the near-field region, which is named as Rayleigh distance, is usually small enough to be neglected. However, when the system is equipped with a large-scale antenna array, the Rayleigh distance might reach tens or even hundreds of meters. This phenomenon has inspired recent studies on near-field communication [9].

Research on near-field communication technology can be mainly classified into two categories. The first category focuses on the performance degradation caused by the unique characteristics of near-field communication systems. Due to the characteristics of spherical wave, some fundamental techniques of current MIMO systems, including channel estimation and beamforming, are no longer suitable for near-field communication. For example, because of the nonlinear phase characteristics of spherical waves in near-field communication, conventional channel estimation methods based on far-field assumptions are no longer applicable. To address this issue, several new codebook designs method for spherical waves were proposed in [10]–[13], based on which the channel estimation scheme techniques were implemented. Another example is the phenomenon of beam split, which has a significant impact and is challenging to deal with in the near field region compared to the far field [14]. To address this problem, a number of effective solutions were proposed in [6], [15].

In contrast, another category of research focuses on utilizing the unique characteristics of near-field propagation to improve the performance of communication systems. For instance, in far-field MIMO communication, the rank of the line-of-sight (LoS) channel matrix is often limited to one, resulting in little spatial degrees of freedom, which limits the spatial multiplexing gain of MIMO systems. Conversely, the spatial degrees of freedom in the near field are significantly increased [16], which provides additional multiplexing gains that can improve the system performance. Based on this additional degree of freedom, new precoding schemes were designed in [17]–[19] to achieve a better performance with a single-user communication scenario.

Recently, it has been found that near field communications have great potential for multi-user scenarios. In multi-user near-field communication systems, the special characteristics of spherical wave provides opportunities for employing multiple access techniques based on the users' location information [20]. In [21], the authors utilized this characteristic to extend

The work K. Cumanan was supported by the UK Engineering and Physical Sciences Research Council (EPSRC) under grant number EP/X01309X/1.

C. Rao and X. Dai are with the CAS Key Laboratory of Wireless-Optical Communications, University of Science and Technology of China, No.96 Jinzhai Road, Hefei, Anhui Province, 230026, P. R. China. (e-mail: rcg1839@mail.ustc.edu.cn; daixc@ustc.edu.cn).

Z. Ding is with Department of Electrical Engineering and Computer Science, Khalifa University, Abu Dhabi, UAE. (e-mail:, zhiguo.ding@ieee.org).

Kanapathippillai Cumanan is with the School of Physics, Engineering and Technology, University of York, York YO10 5DD, U.K. (e-mail: kanapathippillai.cumanan@york.ac.uk)

the space-division multiple access (SDMA), which had already been proposed for far-field communication systems, to the location-division multiple access (LDMA) for near-field communication systems. In general, SDMA can only exploit the azimuth differences between users but cannot utilize the distance differences. Fortunately, LDMA can distinguish between two near-field users located on a same line and introduce the multiplexing gain based on distance differences. The authors also indicated that with an increasing number of antenna elements, two near-field users on the same line can be perfectly distinguished, and the system performance can achieve the ideal upper bound given by Shannon theory. This has opened up a new possibility for exploring the potential of near-field communication. However, in [22], the author found that when the physical parameters of the users and the channel satisfy certain conditions, even with a continuous increase in the number of antenna elements, it is still challenging to perfectly distinguish between two near-field users on the same line. Fortunately, this finding of the inability to distinguish the users allows for the possibility of serving two users with the same beam. Based on this, the author has introduced the concept of resolution, which can measure the ability of distinguishing the near-field users. To utilize the imperfect resolution, non-orthogonal multiple access (NOMA) technique has been exploited in a communication network with poor-resolution near-field users, and achieved a performance improvement. Both works made substantial contributions in the field, but their research perspectives are insufficient for comprehensive analysis due to the lack of effective measurement framework. In [23], the authors have developed a general near-field beam analysis framework based on resolution to analyze and compare the performance of LDMA and NOMA schemes. It has been suggested that by measuring near-field resolution, the base station can determine which scheme is more efficient in achieving a higher performance. However, this study only discussed the two schemes separately and failed to exploit the strengths of both schemes, which motivates our work to use the resolution to utilize the location information between users more flexibly. Specifically, in this paper, an LDMA-NOMA hybrid scheme is proposed, in which the resolution between nearby users can be utilized for beam allocation. LDMA is applied to users with a better resolution, while NOMA is employed for users with a worse resolution. The main contributions of this paper are as follows:

- The resolution of near-field beamforming is applied to analyze and compare the performance of the LDMA-based and NOMA-based schemes, providing a conclusion to determine in which case the LDMA or the NOMA scheme should be applied. This also demonstrates the significance of investigating resolution.
- An LDMA-NOMA hybrid scheme is proposed for a near-field communication scenario. In this scenario, including a new secondary user to an existing LDMA user group is discussed. According to the proposed scheme, the base station treats the secondary user as a NOMA user and serves it with an existing LDMA beam. The comparison of it with conventional LDMA-based schemes is also presented. Additionally, a beam selection method is proposed for the case when existing beams can be adjusted. Specifically, based on the resolution between users, a rule to select a user as a NOMA user for better performance is proposed. To understand the significance of this study, a new evaluation metric, beam efficiency, is introduced and used to assess the performance of the proposed scheme. As the indicator of performance analysis, the closed-form expressions of beam efficiency is obtained.
- Another communication scenario where beam resources are insufficient to serve all users is discussed. Specifically, a resolution-based grouping algorithm is proposed to categorize users into LDMA and NOMA groups. Subsequently, the LDMA-based scheme is applied to allocate beams to serve LDMA users. This approach can make the most utilize of limited beam resources. Simulation results are presented to demonstrate the significant performance improvements of the proposed scheme.

II. Near-Field Beamforming Schemes

In this section, we first describe the model of near-field communication systems. Then we introduce the existing LDMA-based and NOMA-based beamforming schemes, respectively.

A. Near-Field Communication Systems

Consider a base station, (BS), equipped with a UPA with $(2M+1)\times(2N+1)$ elements. The antenna spacing is denoted by d, which is set as $d=\frac{\lambda}{2}$, where λ represents the carrier wavelength. The rectangular coordinates of the UPA elements are given by $\mathbf{s}_{m,n}=(nd,0,md)$, $-M\leq m\leq M$, $-N\leq n\leq N$. BS serves K users, denoted by $\mathrm{U}_1,\mathrm{U}_2,\ldots,\mathrm{U}_K$. The spherical coordinate of U_i is given by $\mathbf{r}_i=(r_i,\theta_i,\phi_i)$. The angles θ_i and ϕ satisfy $0<\theta_i,\phi_i<\pi$. Denote $d_{Ray}=\frac{8d^2(M^2+N^2)}{\lambda}=2\lambda(M^2+N^2)$ as the Rayleigh distance of BS. Then when $r_i\leq d_{Ray}$, the near-field channel model should be adopted. In this paper, it is assumed that $r_i\leq d_{Ray}$ with any $i\in[1,K]$. The channel vector between BS and U_i can be modeled as $\mathbf{h}_i^H=\alpha_i\mathbf{b}_i^H$, where $\alpha_i=\frac{\sqrt{t}\lambda}{4\pi r_i}$ and $\mathbf{b}_i$ represent the channel gain and the response array, respectively. According to the definition of near-field channel model [24], $\mathbf{b}_i$ can be expressed as follows:

$$\mathbf{b}_i=\frac{1}{\sqrt{t}}\Big[e^{-j\frac{2\pi}{\lambda}(||\mathbf{r}_i-\mathbf{s}_{-M,-N}||-r_i)},e^{-j\frac{2\pi}{\lambda}(||\mathbf{r}_i-\mathbf{s}_{-M,-N+1}||-r_i)},\ldots,e^{-j\frac{2\pi}{\lambda}(||\mathbf{r}_i-\mathbf{s}_{M,N}||-r_i)}\Big]^T, \tag{1}$$

where $t=(2M+1)(2N+1)$ represents the normalization coefficient, and $||\cdot||$ represents the Euclidean norm of a vector. Different from far-field communication, the response array of near-field communication users not only depends on the azimuth and elevation angles of users, but also on the distances between users and the base station. This property makes it possible to design new multi-access schemes for near-field communications. An existing LDMA-based scheme, which utilizes the location information to serve multiple users has been proposed, which is introduced in the following subsection.

B. An Existing LDMA-based Scheme

An LDMA-based beamforming scheme was proposed in [21], when there are sufficient beamforming resources, i.e., $N_{RF} \geq K$. Denote N_{RF} as the number of radio frequency (RF) chains equipped at BS. For concise, $N_{RF} = K$ is assumed in this subsection. Denote $\mathbf{x} = \sqrt{P}(\sqrt{l_1}x_1, \sqrt{l_1}x_1, \ldots, \sqrt{l_K}x_K)^T$ as the transmission vector, where P represents the transmission power, $0 < l_1, l_2, \ldots, l_K < 1$ represents the power allocation coefficients, which satisfy $\sum_{k=1}^{K} l_k = 1$. Then the received messages by users can be expressed as follows:

$$\mathbf{y} = \mathbf{HFx} + \mathbf{n}, \tag{2}$$

where $\mathbf{H} = (\mathbf{h}_1, \mathbf{h}_1, \ldots, \mathbf{h}_K)^H$ denotes the channel matrix, $\mathbf{F}$ represents the precoding matrix, and $\mathbf{n}$ is the additive white Gaussian white noise. The precoding matrix usually contains an analog precoder and a digital precoder. Then $\mathbf{F}$ can be expressed as $\mathbf{F} = \mathbf{F}_A\mathbf{F}_D$, where $\mathbf{F}_A \in \mathbb{C}^{t \times N_{RF}}$ and $\mathbf{F}_D \in \mathbb{C}^{N_{RF} \times K}$ represent the analog and digital precoder, respectively. Denote $\mathbf{B} = (\mathbf{b}_1, \mathbf{b}_2, \ldots, \mathbf{b}_K)$ as the response matrix. According to the LDMA-based scheme, the analog precoder is set as $\mathbf{F}_A = \mathbf{B}$, and the digital precoder is set as $\mathbf{F}_D = \bar{\mathbf{H}}^H(\bar{\mathbf{H}}\bar{\mathbf{H}}^H)^{-1}\mathbf{\Lambda}$, where $\bar{\mathbf{H}} = \mathbf{HB}$ represents the effective channel matrix. $\mathbf{\Lambda} = \mathrm{diag}(\lambda_1, \lambda_2, \ldots, \lambda_{0,K})$ is designed to ensure $||\mathbf{F}_A\mathbf{f}_{D,k}||^2 = 1$, where $\mathbf{f}_{D,k}$ is the k-th column of $\mathbf{F}_D$, $1 \leq i \leq K$. From [21], λ_k can be known as

$$\lambda_k = \sqrt{\frac{1}{[(\mathbf{F}_A^H\mathbf{F}_A)^{-1}]_{k,k}}}|\alpha_k|, \tag{3}$$

where $[(\mathbf{F}_A^H\mathbf{F}_A)^{-1}]_{k,k}$ denotes the k-th diagonal element of $(\mathbf{F}_A^H\mathbf{F}_A)^{-1}$. Then the message vector received by users can be expressed as follows:

$$\mathbf{y} = \Lambda\mathbf{x} + \mathbf{n}. \tag{4}$$

The Signal to Interference plus Noise Ratio (SINR) of x_k can be expressed as follows:

$$\gamma_k^L = \frac{\rho\alpha_k^2 l_k}{[(\mathbf{F}_A^H\mathbf{F}_A)^{-1}]_{k,k}}, \tag{5}$$

where $\rho = p/N_0$ represents the signal-noise-ratio (SNR). Then the overall data rate can be expressed as

$$R^L = \sum_{k=1}^{K} \log(1 + \gamma_k^L). \tag{6}$$

According to (5) and (6), $[(\mathbf{F}_A^H\mathbf{F}_A)^{-1}]_{k,k}$ is the key factor of the performance. In [21], the authors believed that as the number of antenna elements $M, N \to +\infty$, $|\mathbf{b}_i^H\mathbf{b}_j| \to 0$ for any $i \neq j$, and

$$\mathbf{F}_A^H\mathbf{F}_A = \begin{pmatrix} 1 & |\mathbf{b}_1^H\mathbf{b}_2|^2 & \ldots & |\mathbf{b}_1^H\mathbf{b}_K|^2 \\ |\mathbf{b}_2^H\mathbf{b}_1|^2 & 1 & \ldots & |\mathbf{b}_2^H\mathbf{b}_K|^2 \\ \vdots & & & \vdots \\ |\mathbf{b}_K^H\mathbf{b}_1|^2 & |\mathbf{b}_K^H\mathbf{b}_2|^2 & \ldots & 1 \end{pmatrix} \to \mathbf{I}_K. \tag{7}$$

In this case, the system's rate will approach the ideal upper bound.

C. An Existing NOMA-based Scheme

A NOMA-based beamforming scheme was proposed for near-field users in [22]. According to the scheme, only one beam is designed to serve all users. The selection of the beam usually depends on the channel fading of users. Without loss of generality, we assume that $\alpha_1 > \alpha_2 > \cdots > \alpha_K$, then the beamforming vector is set as $\mathbf{p}_1$. The transmitted signal vector is expressed as follows:

$$\mathbf{x} = \sqrt{P}\sum_{i=1}^{K} \sqrt{l_i}x_i. \tag{8}$$

Then the message received by U_k is given by

$$\begin{aligned} y_k &= \mathbf{h}_k^H\mathbf{p}_1\mathbf{x} + n_k \\ &= \sqrt{P}\alpha_k^2|\mathbf{b}_k^H\mathbf{b}_1|\sum_{i=1}^{K}\sqrt{l_i}x_i + n_k. \end{aligned} \tag{9}$$

In U_i, successive interference cancellation (SIC) is applied to eliminate $x_{i+1}, x_{i+2}, \ldots, x_K$, then the SINR of x_k can be expressed as follows:

$$\gamma_k^N = \frac{\rho\alpha_k^2|\mathbf{b}_k^H\mathbf{b}_1|^2 l_k}{\rho\alpha_k^2|\mathbf{b}_k^H\mathbf{b}_1|^2\sum_{i=1}^{k-1} l_i + 1}, \tag{10}$$

and the overall data rate can be expressed as

$$R^N = \sum_{k=1}^{K} \log(1 + \gamma_k^N). \tag{11}$$

According to [22], when certain conditions are met, even as the number of antenna elements $M, N \to +\infty$, $|\mathbf{b}_k^H\mathbf{b}_1| > 0$. Therefore, the NOMA-based scheme might work effectively.

However, these two studies did not investigate in which scenarios the scheme should be used. This is due to the lack of a measurement framework. Therefore, in [23], the authors proposed a general framework for near-field beamforming based on the resolutions between users, which is discussed in the next section.

III. Resolution of Near-field Beamforming

One of a potential frameworks for near-field beamforming analysis is named resolution, which is defined as $\Delta_{i,j} = |\mathbf{b}_i^H\mathbf{b}_j|^2$. It can measure the effectiveness of distinguishing the near-field users. From [23], $\Delta_{i,j}$ can be expressed as follows:

$$\Delta_{i,j} \approx \frac{1}{t^2}(\sum_{i=1}^{3} I_i + \frac{I_2 I_3}{t}), \tag{12}$$

where $I_1 = t$,

$$I_2 = 2(2M+1)\sum_{s=1}^{2N}\Phi(z, s, N)\cos(2\pi bs), \tag{13}$$

$$I_3 = 2(2N+1)\sum_{r=1}^{2M}\Phi(c, r, M)\cos(2\pi ar), \tag{14}$$

$$\Phi(x, y, K) = \frac{\sin(2\pi xy(2K - y + 1))}{\sin(2\pi xy)}, \tag{15}$$

$a = \frac{1}{2}(\cos\phi_i - \cos\phi_j)$, $b = \frac{1}{2}(\cos\theta_i \sin\phi_i - \cos\theta_j \sin\phi_j)$, $c = \frac{\lambda}{8}\left(\frac{\sin^2\phi_i}{r_i} - \frac{\sin^2\phi_j}{r_j}\right)$, and $z = \frac{\lambda}{8}\left(\frac{1-\cos^2\theta_i \sin^2\phi_i}{r_i} - \frac{1-\cos^2\theta_j \sin^2\phi_j}{r_j}\right)$.

The physical meaning of $\Delta_{i,j}$ is explained as follows: If $\Delta_{i,j} = 0$, the response vectors of U_i and U_j are orthogonal, indicating that there is no interference between these two users. In this scenario, BS can formulate two separate beams for each user based on their locations without interference, which is referred to as 'perfect resolution'. Conversely,, if $\Delta_{i,j} > 0$, interference will arise between the two beams when using the same beamforming scheme. This situation is called as 'imperfect resolution'. In general, for multi-user case, if $\Delta_{i,j} = 0$ for any $i \neq j$, the resolution of users can be considered perfect, and the LDMA-based scheme performs the best. However, if $\Delta_{i,j} > 0$ for some $i \neq j$, i.e., the resolution is imperfect, the LDMA-based scheme might not perform very well. On the other hand, it makes it possible to use a single beam to serve two or more users at the same time, i.e., the NOMA-based scheme. The question now is, which scheme is better? The answer depends on the locations of users. We can take the case of $K = 2$ as an example to illustrate this answer. As for the LDMA-based scheme, when $K = 2$, $\mathbf{F}_A = (\mathbf{b}_1, \mathbf{b}_2)$, and

$$(\mathbf{F}_A^H \mathbf{F}_A)^{-1} = \begin{pmatrix} (1-\Delta_{1,2})^{-1} & * \\ * & (1-\Delta_{1,2})^{-1} \end{pmatrix}., \quad (16)$$

then R^L can be expressed as follows:

$$R^L = \sum_{k=1}^{2} \log\left(1 + \rho\alpha_k^2 l_k (1-\Delta_{1,2})\right). \quad (17)$$

As for the NOMA-based scheme, when $K = 2$, R^N can be expressed as follows:

$$R^N = \log\left(1 + \rho\alpha_1^2 l_1\right) + \log\left(1 + \frac{\rho\alpha_2^2 \Delta_{1,2} l_2}{\rho\alpha_2^2 \Delta_{1,2} l_1 + 1}\right). \quad (18)$$

Denote $l(\Delta_{1,2}) = \exp(R^N - R^L)$, then

$$l(\Delta_{1,2}) = \frac{1+\rho l_1 \alpha_1^2}{1+\rho l_1 \alpha_1^2 - \rho l_1 \Delta_{1,2} \alpha_1^2} \frac{1+\rho\alpha_2^2\Delta_{1,2}}{1+\rho l_1 \alpha_2^2 \Delta_{1,2}} \times \frac{1}{1+\rho l_2 \alpha_2^2 - \rho l_2 \Delta_{1,2} \alpha_2^2}. \quad (19)$$

When $l(\Delta_{1,2}) \geq 1$, the NOMA scheme is better than LDMA and vice versa. It is obvious that $l(\Delta_{1,2})$ is monotone increasing when $0 \leq \Delta_{1,2} \leq 1$. Therefore, the threshold for $l(\Delta_{1,2})^*) = 1$ can be obtained by using dichotomy. In practice, $l(\Delta_{1,2})$ can be calculated by via (12), and then $l(\Delta_{0,1})$ can be obtained to decide which scheme to adopt.

In the case of high SNR, i.e., when$\rho \to +\infty$, $l(\Delta_{1,2})$ can be approximately simplified as follows:

$$l(\Delta_{1,2}) \approx \frac{1}{1-\Delta_{1,2}} \frac{1}{l_1} \frac{1}{\rho l_2 \alpha_2^2 (1-\Delta_{1,2})}. \quad (20)$$

Then the closed-form approximated solution of $l(\Delta_{1,2}) \geq 1$ can be expressed as follows:

$$\Delta_{1,2} \geq 1 - \frac{1}{\sqrt{\rho l_2 l_1} \alpha_2}, \quad (21)$$

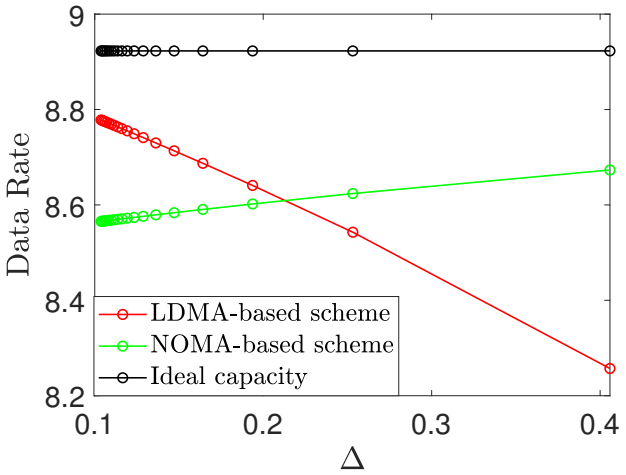

Fig. 1. The data rates of LDMA and NOMA-based schemes with different resolutions.

To better illustrate the impact of resolution on these two schemes, the simulation results of a two-user system are presented as an example in Fig. 1. In the system, one user is fixed while the location of another user is changed. The large scale fading is ignored for fairness. The ideal capacity is also presented for comparison. It can be observed from the figure that the LDMA-based scheme performs well with small Δ, while the performance of the NOMA-based scheme is not that good. As Δ increases, the performance of the LDMA-based scheme becomes worse, while the NOMA-based scheme performs better, which implies that Δ impact significantly on the performance of near-field beamforming communication. It can be noted that both schemes have their own advantages and disadvantages: LDMA can make use of the difference in location information between users, but it will suffer from performance loss caused by resolution reduction. NOMA can utilize the poor resolution for multiplexing, but hard to deal with the interference between users. Therefore, it is meaningful to find a new scheme that can combine the advantages of the two schemes. Based on these two schemes, we propose an LDMA-NOMA hybrid scheme, which can used for various communication scenarios more flexibly and effectively, which is discussed in the next section.

IV. LDMA-NOMA Hybrid Scheme

In this section, we propose a hybrid LDMA-NOMA scheme, and compare it with the conventional LDMA-based scheme. $N_{RF} = K$ is assumed in this section.

A. The Proposed Hybrid LDMA-NOMA Scheme

As shown in Fig. 2, there are K legacy users, denoted by $\mathrm{U}_1, \ldots, \mathrm{U}_K$, which are served by one BS. Denote $\mathbf{h}_k^H = \alpha_k \mathbf{b}_k(r_k, \theta_k, \phi_k)$ as the channel vector of U_k. The LDMA-based scheme is applied for these legacy users, i.e., the beamforming vector for U_k is set as $\mathbf{p}_k = \mathbf{b}_k$. Now an additional

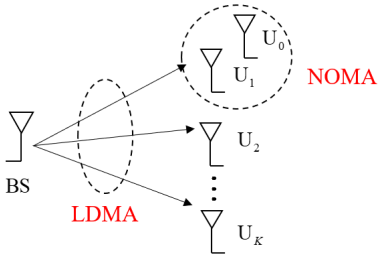

Fig. 2. The system model of hybrid LDMA-NOMA scheme.

secondary user[1] U_0 needs to be served by this system. Then BS can serve U_0 via an existing beam, which is chosen according to the resolutions between users. Without loss of generality, it is assumed that $\Delta_{0,1} \geq \Delta_{0,2} \geq \cdots \geq \Delta_{0,K}$. Then the closest beam to U_0, i.e., U_1 is selected to ride on.

Denote $\mathbf{H} = (\mathbf{h}_1, \ldots, \mathbf{h}_K)^H$ as the channel matrix for LDMA users. The analog precoder for the LDMA users is set as $\mathbf{F}_A = (\mathbf{b}_1, \ldots, \mathbf{b}_K)$. The design of digital precoder $\mathbf{F}_D$ and the diagonal matrix $\mathbf{\Lambda}$ is similar to the LDMA-based scheme, which is expressed as $\mathbf{F}_D = \bar{\mathbf{H}}^H(\bar{\mathbf{H}}\bar{\mathbf{H}}^H)^{-1}\mathbf{\Lambda}$, $\bar{\mathbf{H}} = \mathbf{H}\mathbf{F}_A$, $\mathbf{\Lambda} = \mathrm{diag}(\lambda_1, \ldots, \lambda_K)$, and

$$\lambda_k = \sqrt{\frac{1}{[(\mathbf{F}_A^H\mathbf{F}_A)^{-1}]_{k,k}}}|\alpha_k|. \tag{22}$$

The transmitted signal vector from the BS is given by

$$\mathbf{x} = \mathbf{F}_A\mathbf{F}_D\mathbf{x}^L + \sqrt{P}\mathbf{p}_0\sqrt{l_0}x_0, \tag{23}$$

where $\mathbf{x}^L = \sqrt{P}(\sqrt{l_1}x_1, \ldots, \sqrt{l_K}x_K)^T$ represents the signals intended for the LDMA users, and $\mathbf{p} \in \{\mathbf{b}_1, \ldots, \mathbf{b}_K\}$ represents the beamforming vector for U_i^N. Then the message received by LDMA users can be expressed as follows:

$$y_k = \sqrt{P}\left(\lambda_k\sqrt{l_k}x_k + \alpha_k\sqrt{\Delta_k, 1}\sqrt{l_0}x_0\right) + n_k. \tag{24}$$

The SIC is adopted in LDMA users to eliminate the interference x_0, then the SINR of $x_k, k \geq 1$ can be expressed as follows:

$$\gamma_k = \rho\lambda_k^2 l_k = \frac{\rho\alpha_k^2 l_k}{[(\mathbf{F}_A^H\mathbf{F}_A)^{-1}]_{k,k}}. \tag{25}$$

The message received by U_0 is expressed as follows:

$$\begin{aligned} y_0 &= \mathbf{h}_0^H\mathbf{F}_A\mathbf{F}_D\mathbf{x}^L + \mathbf{h}_0^H\sqrt{P}\mathbf{b}_1\sqrt{l_0}x_0 + n_0 \\ &= \sqrt{P}\left(\alpha_0\sqrt{\Delta}_{0,1}\sqrt{l_0}x_l^N + \alpha_0\mathbf{h}_0^H\sum_{j=1}^{K}\mathbf{F}_A\mathbf{f}_{D,j}\sqrt{l_j}x_j\right) \\ &\quad + n_0, \end{aligned} \tag{26}$$

The SINR of x_0 can be expressed as follows:

$$\begin{aligned} \gamma_0 &= \frac{\rho\alpha_0^2\Delta_{0,1}l_0}{\rho\sum_{j=1}^{K}|\mathbf{h}_0^H\mathbf{F}_A\mathbf{f}_{D,j}|^2 l_j + 1} \\ &= \frac{\rho\alpha_0^2\Delta_{0,1}l_0}{\rho\alpha_0^2\sum_{j=1}^{K}\lambda_j^2\Delta_{0,j}l_j + 1}, \end{aligned} \tag{27}$$

[1]A secondary user refers to a new user added to the communication system, as opposed to the legacy users who are already part of the system. This concept is similar to the one introduced in [25].

The overall rate of the system is given by

$$R^H = \sum_{k=1}^{K}\log(1+\gamma_k) + \log(1+\gamma_0). \tag{28}$$

B. The Comparison of the proposed hybrid LDMA-NOMA scheme and LDMA-based scheme

Another available option is to formulate a new beam for U_0 and apply the LDMA to all users. Denote $\mathbf{H}_0 = (\mathbf{h}_0, \ldots, \mathbf{h}_K)^H$ as the channel matrix. According to the LDMA scheme, the analog precoder is set as $\mathbf{F}_{A,0} = (\mathbf{b}_0, \mathbf{F}_A) = (\mathbf{b}_0, \ldots, \mathbf{b}_K)$, and the digital precoder is set as $\mathbf{F}_{D,0} = \bar{\mathbf{H}}_0^H(\bar{\mathbf{H}}_0\bar{\mathbf{H}}_0^H)^{-1}\mathbf{\Lambda}_0$, where $\bar{\mathbf{H}}_0 = \mathbf{H}_0\mathbf{F}_{A,0}$ is the effective channel matrix. $\mathbf{\Lambda}_0 = \mathrm{diag}(\lambda_{0,1}, \ldots, \lambda_{0,K})$ is designed to ensure $||\mathbf{F}_{A,0}\mathbf{f}_{D,0,i}||^2 = 1$, where $\mathbf{f}_{D,0,i}$ is the i-th column of $\mathbf{F}_{D,0}$, $1 \leq i \leq k$. From [21], λ_k can be known as

$$\lambda_k = \sqrt{\frac{1}{[(\mathbf{F}_{A,0}^H\mathbf{F}_{A,0})^{-1}]_{k,k}}}|\alpha_k|, \tag{29}$$

where $[(\mathbf{F}_{A,0}^H\mathbf{F}_{A,0})^{-1}]_{k,k}$ denotes the k-th diagonal element of $(\mathbf{F}_{A,0}^H\mathbf{F}_{A,0})^{-1}$. The transmitted signal sent by BS is given by

$$\mathbf{x} = \mathbf{F}_{A,0}\mathbf{F}_{D,0}\mathbf{x}_0^L, \tag{30}$$

where $\mathbf{x}_0^L = \sqrt{P}(\sqrt{l_0}x_0, \ldots, \sqrt{l_K}x_K)^T$ represents the signals intended for the users. $0 < l_k < 1$ represents the power allocation coefficient of the k th user and satisfies $\sum_{k=0}^{K} l_k = 1$. Then the message vector received by users can be expressed as follows:

$$\mathbf{y}^L = \mathbf{H}\mathbf{x} + \mathbf{n} = \Lambda\mathbf{x} + \mathbf{n}. \tag{31}$$

The SINR of x_k can be expressed as follows:

$$\gamma_k^L = \frac{\rho\alpha_k^2 l_k}{[(\mathbf{F}_{A,0}^H\mathbf{F}_{A,0})^{-1}]_{k,k}}, \tag{32}$$

where $\rho = p/N_0$ represents the SNR. Then the sum rate can be expressed as follows:

$$R^L = \sum_{k=0}^{K}\log(1+\gamma_k^L). \tag{33}$$

The data rate is used as an indicator to compare the performance of the two schemes. By solving $R^H - R^L \geq 0$, it can be realized that

$$\Delta_{0,1} \geq \frac{\rho\sum_{j=1}^{K}|\mathbf{h}_0^H\mathbf{F}_A\mathbf{f}_{D,j}|^2 l_j + 1}{\rho\alpha_0^2 l_0}\left(\frac{1}{g(\mathbf{F}_A, \mathbf{b}_0)} - 1\right), \tag{34}$$

where

$$\begin{aligned} g(\mathbf{F}_A, \mathbf{b}_0) &= \frac{1}{1 + \frac{\rho\alpha_0^2 l_0}{[(\mathbf{F}_{A,0}^H\mathbf{F}_{A,0})^{-1}]_{1,1}}} \\ &\quad \times \prod_{k=1}^{K}\frac{1 + \frac{\rho\alpha_k^2 l_k}{[(\mathbf{F}_A^H\mathbf{F}_A)^{-1}]_{k,k}}}{1 + \frac{\rho\alpha_k^2 l_k}{[(\mathbf{F}_{A,0}^H\mathbf{F}_{A,0})^{-1}]_{k+1,k+1}}}. \end{aligned} \tag{35}$$

Denote

$$f(\Delta_{0,1}) = \Delta_{0,1} - \frac{\rho\alpha_0^2 \sum_{j=1}^{K} \lambda_j^2 \Delta_{0,j} l_j + 1}{\rho\alpha_0^2 l_0} \left(\frac{1}{g(\mathbf{F}_A, \mathbf{b}_0)} - 1 \right). \tag{36}$$

When $f(\Delta_{0,1}) \geq 0$, the NOMA scheme is better than LDMA and vice versa. This condition can be used to decide which scheme to adopt. From (36), it can be seen that the value of $f(\Delta_{0,1})$ depends on the locations of users, which is discussed through the following corollary.

Corollary 1. *When $\mathbf{b}_0$ is a linear combination of $\mathbf{b}_1 \sim \mathbf{b}_k$, the proposed LDMA-NOMA hybrid scheme reaches the highest performance.*

Proof. Since $\mathbf{F}_{A,0} = (\mathbf{b}_0, \mathbf{F}_A)$, we can express $(\mathbf{F}_{A,0}^H \mathbf{F}_{A,0})^{-1}$ with $\mathbf{F}_A$ and $\mathbf{b}_0$ via block matrix computation as follows:

$$(\mathbf{F}_{A,0}^H \mathbf{F}_{A,0})^{-1} = \begin{pmatrix} (1 - \mathbf{b}_0^H \mathbf{F}_A (\mathbf{F}_A^H \mathbf{F}_A)^{-1} \mathbf{F}_A^H \mathbf{b}_0)^{-1} & * \\ * & (\mathbf{F}_A^H (\mathbf{I} - \mathbf{b}_0 \mathbf{b}_0^H) \mathbf{F}_A)^{-1} \end{pmatrix}. \tag{37}$$

Then it can be seen that $[(\mathbf{F}_{A,0}^H \mathbf{F}_{A,0})^{-1}]_{1,1} = (1 - \mathbf{b}_0^H \mathbf{F}_A (\mathbf{F}_A^H \mathbf{F}_A)^{-1} \mathbf{F}_A^H \mathbf{b}_0)^{-1}$. To satisfy (34), it is necessary to make the right side of the inequality as small as possible, i.e., it is necessary to make $(\mathbf{F}_{A,0}^H \mathbf{F}_{A,0})^{-1}$ as large as possible. To make $[(\mathbf{F}_{A,0}^H \mathbf{F}_{A,0})^{-1}]_{0,0}$ as large as possible, the problem can be formulated as follows:

$$\begin{aligned} &\max \{ \mathbf{b}_0^H \mathbf{F}_A (\mathbf{F}_A^H \mathbf{F}_A)^{-1} \mathbf{F}_A^H \mathbf{b}_0 \} \\ &\text{s.t. } \mathbf{b}_0^H \mathbf{b}_0 = 1. \end{aligned} \tag{38}$$

This is a problem about principle component analysis [26], which returns the possible solutions of the eigenvectors of $\mathbf{F}_A (\mathbf{F}_A^H \mathbf{F}_A)^{-1} \mathbf{F}_A^H$, i.e., $\mathbf{F}_A (\mathbf{F}_A^H \mathbf{F}_A)^{-1} \mathbf{F}_A^H \mathbf{b}_0^* = \lambda \mathbf{b}_0^*$, and $\mathbf{F}_A (\mathbf{F}_A^H \mathbf{F}_A)^{-1} \mathbf{F}_A^H = \lambda$. Notice that $\mathbf{F}_A (\mathbf{F}_A^H \mathbf{F}_A)^{-1} \mathbf{F}_A^H$ is the projection matrix of $\mathbf{F}_A$, λ is either 0 or 1. It is obvious that $\lambda = 0$ is not the solution. Therefore, when $\lambda = 1$, i.e., when $\mathbf{b}_0$ is a linear combination of $\mathbf{b}_1 \sim \mathbf{b}_K$, the proposed hybrid LDMA-NOMA scheme has the greatest advantage over the LDMA-based scheme. □

Remark 1. *The result in Corollary 1 is also physically intuitive. $\mathbf{b}_0$ is a linear combination of $\mathbf{b}_1 \sim \mathbf{b}_K$ means that the resolution between U_0 and K legacy users is poor. This makes it challenging to distinguish U_0 and legacy users, resulting in a lower performance for the LDMA-based scheme. On the contrary, when $\mathbf{b}_1$ is orthogonal to $\mathbf{b}_1 \sim \mathbf{b}_K$, the LDMA-based scheme reaches the highest performance. In other cases, it can be measured by the angle between $\mathbf{b}_0$ and span$\{\mathbf{b}_1, \mathbf{b}_2, \ldots, \mathbf{b}_K\}$, which can be expressed as follows:*

$$\theta(\mathbf{b}_0, \mathbf{B}) = \arccos ||\mathbf{B}(\mathbf{B}^H \mathbf{B})^{-1} \mathbf{B}^H \mathbf{b}_0||^2. \tag{39}$$

Lower $\theta(\mathbf{b}_0, \mathbf{B})$ means a smaller distance between $\mathbf{b}_0$ and span$\{\mathbf{b}_1, \mathbf{b}_2, \ldots, \mathbf{b}_K\}$, and means a better performance of LDMA-NOMA hybrid scheme. This result can be used as a simple judgment for deciding which option to adopt.

Remark 2. *From the analysis above, the proposed hybrid scheme is not always better than the LDMA-based scheme when the rate is used as the indicator. However, the hybrid scheme can reserve the beam resource. To show this advantage, we define a new indicator η, named beam efficiency, which is defined as*

$$\eta = \frac{\textit{Rate}}{\textit{The number of used beam}}. \tag{40}$$

It is important to note that the unit of beam efficiency is the same as that of the rate. Then the beam efficiency of the two schemes can be respectively expressed as follows:

$$\eta^N = \frac{R^N}{K}, \eta^L = \frac{R^L}{K+1}. \tag{41}$$

It can be seen that the proposed hybrid scheme has more advantages in beam efficiency.

SNR is also an important factor in communication systems. To study the performance of the two schemes with high or low SNR environments, the following corollary is given.

Corollary 2. *When $\rho \to +\infty$,*

$$f(\Delta_{0,1}) \to \Delta_{0,1} - C_1 \rho + C_2, \tag{42}$$

where $C_1, C_2 > 0$ are constants independent of ρ.

On the contrary, when $\rho \to 0$,

$$f(\Delta_{0,1}) \to \Delta_{0,1} - (1 - \mathbf{b}_0^H \mathbf{F}_A (\mathbf{F}_A^H \mathbf{F}_A)^{-1} \mathbf{F}_A^H \mathbf{b}_0). \tag{43}$$

Proof. See Appendix A. □

Remark 3. *From Corollary 2, it can be known that with the high SNR environment, the LDMA-based scheme performs well. When SNR is low, it depends on the locations of users, i.e., if the response vector of $\mathbf{b}_0$ is closely related to the response vectors of other users, the value of $(1 - \mathbf{b}_0^H \mathbf{F}_A (\mathbf{F}_A^H \mathbf{F}_A)^{-1} \mathbf{F}_A^H \mathbf{b}_0)$ is smaller, and the LDMA-NOMA hybrid scheme performs well.*

C. The Improved Scheme with Beam Selection

In the scheme proposed in Subsection IV-A, the exiting beams are fixed and cannot be changed. However, if BS can decide which user to be a "NOMA user" and others to be "LDMA users" from all $K+1$ users, rather than using the existing beams from K legacy users directly, the performance might be better. The problem can be described as follows: Choose a "NOMA user" U_N from $\mathrm{U}_0, \mathrm{U}_1, \ldots, \mathrm{U}_K$, and regards it as the secondary user. The remaining users are regarded as legacy users, then apply the LDMA-NOMA hybrid scheme to the users. Notice that the performance of the LDMA or NOMA scheme depends on the resolution Δ, smaller Δ tends to choose the LDMA scheme while larger Δ prefers NOMA. Therefore, BS can choose the "NOMA user" depending on the resolutions. Specifically, to better quantify and compare the resolution of each user with all other users, let us define the sum resolution $S(i)$ as

$$S(i) = \sum_{j=0, j \neq i}^{K} \Delta_{i,j}. \tag{44}$$

Then BS can choose U_N as

$$\mathrm{U}_N = \arg \max_{0 \leq N \leq K} S(N). \tag{45}$$

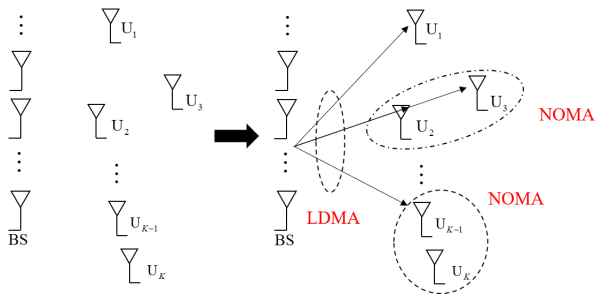

Fig. 3. The user grouping scheme.

Once BS has selected U_N, BS can apply the LDMA-based scheme to $\mathrm{U}_0, \mathrm{U}_1, \ldots, \mathrm{U}_{N-1}, \mathrm{U}_{N+1}, \ldots, \mathrm{U}_K$ and formulate $K-1$ beams. And then choose the closest beam to serve U_N and with the NOMA-based scheme. The performance of the scheme can be obtained by setting $\mathbf{F}_A = \mathbf{B}_N$ and replacing $\mathbf{b}_0$ with $\mathbf{b}_N$ in (28).

The complexity of this method can be easily determined. It requires K calculations of $S(i)$, where each $S(i)$ involves $K-1$ computations. Additionally, it is necessary to compute $\Delta_{i,j}$ for any $1 \le i < j \le K$, which involves a total of $K(K-1)/2$ resolution calculations. From 12, the number of calculations required to obtain the resolution is given by $2(M+N)$. Therefore, the total complexity is $K(K-1)(M+N+1) \approx K^2(M+N)$.

Remark 4. *This discussion shows that adding a new user to the existing near-field LDMA network may have a better or worse performance with the NOMA-LDMA scheme than with LDMA-based scheme. This discussion considers the case of sufficient beam resources (enough RF chains, see [21]). However, when the beam resources are less than the total number of users, the NOMA-LDMA scheme should be used. At this point, how to allocate the limited beam to users reasonably is a significant problem, which will be discussed in the next section.*

V. The LDMA-NOMA Hybrid Scheme For the Case With Lack of Beam Resources

Consider K users, which are denoted by $\mathrm{U}_1, \ldots, \mathrm{U}_K$, served by BS. Limited by the beam resources, only $N_{RF} = K_L < K$ RF chains are available, i.e., only K_L beams can be designed. Therefore, it is necessary to divide the users into two groups $\mathcal{U}^L$ and $\mathcal{U}^N$. After the user grouping, BS formulates K_L beams for all users in $\mathcal{U}^L$ according to the LDMA-based scheme. Then BS chooses a beam for each user in $\mathcal{U}^N$ to apply NOMA-based scheme. Denote U_i^L and U_j^N as the i-th and j-th user in $\mathcal{U}^L$ and $\mathcal{U}^N$, respectively. The performance significantly depends on the grouping strategy. An efficient grouping strategy is discussed in this section.

A. User Grouping

The approach is to extend the method in Subsection IV-C to the multi-user case, which is illustrated in Fig. 3. Specifically, BS chooses the user with the maximum S as the first user for $\mathcal{U}^N$. Then BS continues to choose the second user from the remaining users with the same process until the number of elements in $\mathcal{U}^N$ becomes $1-K_L$. After obtaining $\mathcal{U}^L$, BS can design the beamforming vectors as the response vectors of users in $\mathcal{U}^L$. Then the nearest beam is chosen to serve each user in $\mathcal{U}^N$. Define a multi-valued mapping $\mathbf{g}(j) : [1, K_L] \to [1, K_N]$ to describe the pairing situation by the rule that the j-th beam serves $\mathrm{U}_{g(j)}^N$, i.e., $\mathbf{p}_{g(j)}^N = \mathbf{b}_j^L$, where $g(j) \in \mathbf{g}(j)$. Denote $\Delta_{i,j}^{\xi_1,\xi_2} = |\mathbf{b}_i^{\xi_1 H} \mathbf{b}_j^{\xi_2}|^2$, $\xi_1, \xi_2 \in \{L, N\}$ as the resolution between $\mathrm{U}_i^{\xi_1}$ and $\mathrm{U}_j^{\xi_2}$. Then the overall grouping and pairing strategy is provided in Algorithm V-A.

Algorithm 1 User Grouping and Pairing Algorithm

Input: The location information of $\mathrm{U}_1, \ldots, \mathrm{U}_K$, K_L, M, N.
Output: User groups $\mathcal{U}^L$, $\mathcal{U}^N$, and pairing map $\mathbf{g}()$.

For any $1 \le i < j \le K$, obtain $\Delta_{i,j}$ according to (12).
For any $1 \le i \le K$, obtain $S(i)$ according to (44).
for $\updownarrow(\mathcal{U}^N) \le K_N$ **do**
  Choose $\mathrm{U}_N = \arg \max_{0 \le N \le K} S(N)$, add U_N to $\mathcal{U}^N$.
  $j = 1$
  for $j \le K$ **do**
    $S(j) = S(j) - \Delta_{j,N}$.
    $j = j + 1$.
  Add U_N to $\mathcal{U}^N$.
Add all remaining users to $\mathcal{U}^L$.
Set $i = 1$.
for $i \le K_N$ **do**
  Find j^* that satisfies $\Delta_{i,j^*}^{N,L} = \max_{1 \le j \le K_L} \Delta_{i,j}^{N,L}$.
  Add a new value i for $\mathbf{g}(j^*)$.
  $i = i + 1$.
return $\mathcal{U}^L$, $\mathcal{U}^N$, $\mathbf{g}()$.

The complexity can be easily obtained. According to the analysis in Subsection IV-C, the complexity of Step 1 and 2 is $K(K-1)(M+N)+K-1$. Steps 3 to 6 require $2KK_N$ computations, while the remaining steps involve $K_N K_L$ computations. Consequently, the total complexity is given by $K(K-1)(M+N)+K-1+2KK_N+K_NK_L \approx K^2(M+N)$, which is similar to the case in Section IV.

The performance of proposed algorithm will be presented in the following subsection.

B. Performance Analysis

Denote $\mathcal{U}^L = \{\mathrm{U}_1^L, \ldots, \mathrm{U}_{K_L}^L\}$, $\mathcal{U}^N = \{\mathrm{U}_1^N, \ldots, \mathrm{U}_{K_N}^N\}$, $K = K_L + K_N$. The channel vector of U_i^ξ is denoted by $\mathbf{h}_i^{\xi H} = \alpha_i^\xi \mathbf{b}_i^{\xi H}$, where $\xi \in \{L, N\}$. $\mathbf{H}^\xi = (\mathbf{h}_1^\xi, \ldots, \mathbf{h}_{K_\xi}^\xi)^H$ represents the channel matrix. Then the analog precoder for the LDMA users is set as $\mathbf{F}_A = (\mathbf{b}_1^L, \ldots, \mathbf{b}_{K_L}^L)$, and the digital precoder is set as $\mathbf{F}_D = \bar{\mathbf{H}}^H(\bar{\mathbf{H}}\bar{\mathbf{H}}^H)^{-1}\mathbf{\Lambda}$, where $\bar{\mathbf{H}} = \mathbf{H}\mathbf{F}_A$ is the effective channel matrix. $\mathbf{\Lambda} = \mathrm{diag}(\lambda_1, \ldots, \lambda_{K_L})$ is designed to ensure $||\mathbf{F}_A \mathbf{f}_{D,i}||^2 = 1$, where $\mathbf{f}_{D,i}$ is the i-th column of $\mathbf{F}_D$, $1 \le i \le k$. From [21], λ_j can be known as

$$\lambda_j = \sqrt{\frac{1}{[(\mathbf{F}_A^H \mathbf{F}_A)^{-1}]_{j,j}}} |\alpha_j^L|, \tag{46}$$

where $[(\mathbf{F}_A^H\mathbf{F}_A)^{-1}]_{j,j}$ denotes the j-th diagonal element of $(\mathbf{F}_A^H\mathbf{F}_A)^{-1}$.

The message sent by BS is given by

$$\mathbf{x} = \mathbf{F}_A\mathbf{F}_D\mathbf{x}^L + \sqrt{P}\sum_{i=1}^{K_N}\mathbf{p}_i^N\sqrt{l_i^N}x_i^N, \tag{47}$$

where $\mathbf{x}^L = \sqrt{P}(\sqrt{l_1^L}x_1^L, \ldots, \sqrt{l_{K_L}^L}x_{K_L}^L)^T$ represents the signals intended for the LDMA users, x_i^N and $\mathbf{p}_i^N \in \{\mathbf{b}_1^L, \ldots, \mathbf{b}_{K_L}^L\}$ represent the signal and the beamforming vector for U_i^N, respectively. Then the received signal vector by LDMA users can be expressed as follows:

$$\mathbf{y}^L = \mathbf{H}\mathbf{x} + \mathbf{n} = \Lambda\mathbf{x} + \sqrt{\frac{P}{K}}\sum_{i=1}^{K_N}\mathbf{H}\mathbf{p}_i^N\sqrt{l_i^N}x_i^N + \mathbf{n}. \tag{48}$$

Then the message received by U_j^L can be expressed as follows:

$$\begin{aligned} y_j^L = \sqrt{P}(&\lambda_j\sqrt{l_j^L}x_j^L + \sum_{g\in\mathbf{g}(j)}\alpha_j^L\sqrt{l_g^N}x_g^N \\ &+ \alpha_j^L\sum_{i=1,i\notin\mathbf{g}(j)}^{K_N}\sqrt{\Delta_{j,g^{-1}(i)}^{L,L}}\sqrt{l_i^N}x_i^N) + n, \end{aligned} \tag{49}$$

where $g^{-1}()$ denotes the inverse mapping of $\mathbf{g}()$.The SIC is adopted in U_j^L to eliminate the interference caused by the users from $\mathcal{U}^N$, then the SINR of x_j^L can be expressed as follows:

$$\gamma_j^L = \rho\lambda_j^2 l_j^L = \frac{\rho\alpha_j^{L2}l_j^L}{[(\mathbf{F}_A^H\mathbf{F}_A)^{-1}]_{j,j}}, \tag{50}$$

where $\rho = P/N_0$ represents the SNR. Similarly, the message received by U_l^N can be expressed as follows:

$$\begin{aligned} y_l^N &= \mathbf{h}_l^{NH}\mathbf{F}_A\mathbf{F}_D\mathbf{x}^L + \mathbf{h}_l^{NH}\sqrt{\frac{P}{K}}\sum_{i=1}^{K_N}\mathbf{p}_i^N\sqrt{l_i^N}x_i^N + n \\ &= \sqrt{P}(\alpha_l^N\sqrt{\Delta_{l,g^{-1}(l)}^{N,L}}\sqrt{l_l^N}x_l^N + \alpha_l^N\mathbf{h}_l^{NH}\sum_{j=1}^{K_L}\mathbf{F}_A\mathbf{f}_{D,j}x_j^L \\ &+ \sum_{i=1,i\neq l}^{K_N}\sqrt{\Delta_{l,g^{-1}(i)}^{N,L}}\sqrt{l_i^N}x_i^N) + n, \end{aligned} \tag{51}$$

where and $\mathbf{f}_{D,j}$ represents the j-th column of $\mathbf{F}_D$. SIC is adopted in the NOMA users in sequence to eliminate the other NOMA users' message.

NOMA users decode their own messages directly, and the SINR of x_l^N can be expressed as follows:

$$\gamma_l^N = \frac{\rho\alpha_l^{N2}\Delta_{l,g^{-1}(l)}^{N,L}l_l^N}{I_l}, \tag{52}$$

where

$$\begin{aligned} I_l =&\rho\alpha_l^{N2}\sum_{j=1}^{K_L}|\mathbf{b}_l^{NH}\mathbf{F}_A\mathbf{f}_{D,j}|^2 l_j^L \\ &+ \rho\alpha_l^{N2}\sum_{i=1,i\neq l,i\notin\mathbf{h}(l)}^{K_N}\Delta_{l,g^{-1}(i)}^{N,L}l_i^N + 1 \\ =&\rho\alpha_l^{N2}\sum_{j=1}^{K_L}\lambda_j^2\Delta_{l,j}^{N,L}l_j \\ &+ \rho\alpha_l^{N2}\sum_{i=1,i\neq l,i\notin\mathbf{h}(l)}^{K_N}\Delta_{l,g^{-1}(i)}^{N,L}l_i^N + 1, \end{aligned} \tag{53}$$

$\mathbf{h}(l)$ denotes a set that each element i in $\mathbf{h}(l)$ needs to satisfy the following two conditions:

$$\begin{aligned} &g^{-1}(i) = g^{-1}(l) \\ &|\mathbf{h}_i^N| < |\mathbf{h}_l^N|. \end{aligned} \tag{54}$$

The overall rate of the system is given by

$$R = \sum_{j=1}^{K_L}\log(1+\gamma_j^L) + \sum_{l=1}^{K_N}\log(1+\gamma_l^N). \tag{55}$$

The beam efficiency can be obtained by $\eta = \frac{R}{K_L}$. To study the performance with high or low SNR environment, the following corollary is given.

Corollary 3. *When $\rho \to +\infty$, $R \sim K_S\log(\rho)$, where $K_L \leq K_S \leq K_L + K_{beam}$ depends on the users. K_{beam} denotes the number of beams that carry any NOMA user.*

Proof. See Appendix B. □

Remark 5. *From Corollary 3, it can be seen that the increased rate of R with increasing SNR is related to the total number of beams and the number of beams carrying NOMA users. Considering the balance with beam efficiency, when k_L is small, it is better to maximize K_{beam} as much as possible to achieve optimal performance. Maximizing K_{beam} implies that the resolution between each NOMA user is good, which may provide a reference for further optimizing the grouping strategy.*

VI. Simulation

In this section, the simulation results are presented. The carrier frequency is set as $f = 30$ Ghz, and thus wavelength is $\lambda = 10^{-2}$ m. The antenna spacing is chosen as $d = \frac{\lambda}{2} = 5\times10^{-3}$ m. The simulations in this paper has not considered large-scale fading.

Fig. 4 illustrates the overall rate of the proposed LDMA-NOMA hybrid scheme, alongside the results of the LDMA-based scheme for comparison. The antenna array size is set to $M = N = 32$. There are $K = 40$ legacy users uniformly distributed along four straight lines with azimuth angles of $\theta_1 = -\pi/3, \theta_2 = -\pi/9, \theta_3 = \pi/9, \theta_4 = \pi/3, \phi = \pi/6$. The users are distributed along the lines with a range of 2.1 m to 9.4 m. The additional user is placed at two different angles, $\theta_0 = 0$ and $\theta_0 = \pi/9$, respectively, with a radial

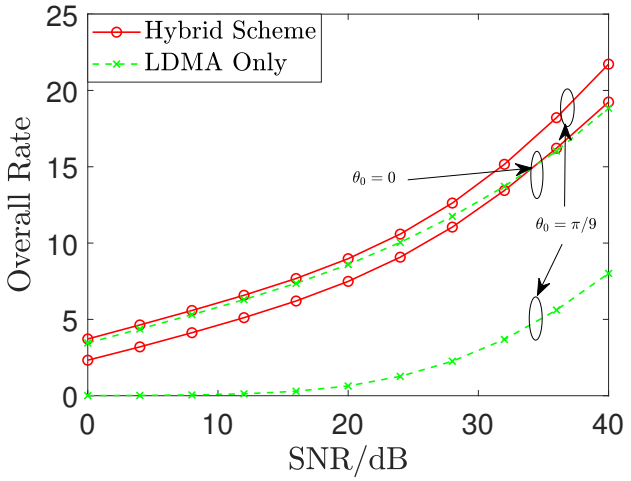

Fig. 4. Comparison of the proposed scheme and LDMA-based scheme in terms of overall rate.

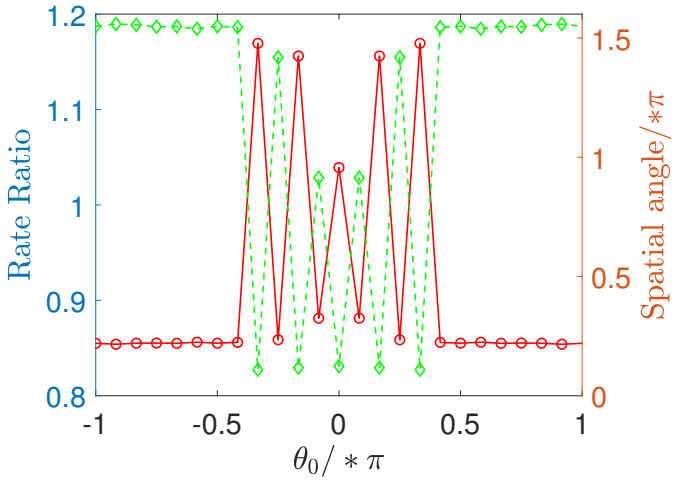

Fig. 5. Comparison between the proposed LDMA-NOMA hybrid scheme and the LDMA-based scheme and their relationship with the angle between the beam vectors. The red line marked with circles represents rate ratio R^N/R^L, while the green line marked with diamonds represents the spatial angle $\theta(\mathbf{b}_0, \mathbf{B}) = \arccos ||\mathbf{B}(\mathbf{B}^H\mathbf{B})^{-1}\mathbf{B}^H\mathbf{b}_0||^2$. The unit of the horizontal and right-hand vertical axis represents the multiple of pi.

distance of $r_0 = 3.27$ m. It can be observed that when $\theta_0 = \pi/9$, i.e., the additional user is at a same line with a group of legacy users, the proposed hybrid scheme performs better than LDMA-based scheme. The reason is the poor resolutions between the additional user and legacy users in this case. However, when $\theta_0 = 0$, the additional user is more easily distinguishable, thus the LDMA-based scheme performs better. This result suggests that the proposed hybrid scheme does not always perform better than the LDMA-based scheme. Its performance advantage depends on the spatial distribution of users, as discussed in Remark 2.

To study the relationship between the performance of the proposed scheme and user locations, Fig. 5 illustrates the variation of rate with the change in the positions of secondary users while the positions of legacy users are fixed. The elevation angle of the 5 legacy users is fixed at $\phi_i = \pi/6$, with azimuth angles uniformly distributed in the range of $[-\pi/3, \pi/3]$, and they are located at a distance of 24.6 m from the base station. The elevation angle of the secondary user is also fixed at $\phi_0 = \pi/6$, located at a distance of 12.3 m from the base station, while its azimuth angle θ_0 varies. The ratio of rates between the two schemes R^N/R^L are plotted in Fig. 5, marked by circular symbols and red lines. Additionally, the angle $\theta(\mathbf{b}_0, \mathbf{B})$ between the beam vector of the secondary user and the subspace formed by the beam vectors of legacy users is presented in the Fig. 5, marked by diamond symbols and green lines. The number of antennas is set to $M = N = 32$, while the SNR is chosen as $\rho = 40$ dB. From the figure, it can be seen that the rate ratio fluctuates significantly with θ_0, indicating that the performance is influenced by the angle of the secondary user. This is because that the angle determines its resolution concerning other users. Moreover, the angle $\theta(\mathbf{b}_0, \mathbf{B})$ is found to be inversely correlated with the rate ratio, i.e., a higher rate is achieved when the angle is smaller, indicating the superiority of the LDMA-NOMA hybrid scheme, while the advantage is less outstanding when the angle is larger. This aligns with the conclusion drawn in Fig. 1. Hence, in practice, this angle can be utilized to determine which scheme to choose.

Fig. 6 presents the beam efficiency of the proposed LDMA-NOMA hybrid scheme and compares it with that of the LDMA-based scheme. Additionally, the results of an improved scheme based on user selection are also shown in the same figure. Three different user distribution scenarios are considered:

- All users are uniformly distributed along a single straight line with an azimuth angle of $\theta_1 = -\frac{\pi}{6}, \theta_2 = \frac{\pi}{6}, \phi = \frac{\pi}{6}$.
- All users are uniformly distributed along two straight lines with azimuth angles of $\theta_1 = -\frac{\pi}{3}$ and $\theta_2 = \frac{\pi}{3}$.
- All users are uniformly distributed along four straight lines with azimuth angles of $\theta_1 = -\frac{\pi}{3}, \theta_2 = -\frac{\pi}{9}, \theta_3 = \frac{\pi}{9}, \theta_4 = \frac{\pi}{3}, \phi = \frac{\pi}{6}$.

The users are distributed along the lines within a range of 8.2 m to 21.3 m. The number of antennas is set to $M = N = 32$. Results for different numbers of users K are shown in the figure. It can be observed from the figure that the proposed LDMA-NOMA hybrid scheme achieves higher beam efficiency compared to that of the LDMA-based scheme. The scheme with user selection can further increase the beam efficiency. This demonstrates the superiority of the proposed scheme in this paper. Specifically, from Subfigure (a), it can be observed that when all users are distributed along a single straight line, the beam efficiency of the LDMA-based scheme is almost zero. The proposed LDMA-NOMA hybrid scheme significantly improves beam efficiency in this case. This is because the resolution between adjacent users is very poor, making it nearly impossible to distinguish between these users, which leads to a poor performance of the LDMA-based scheme. However, this poor resolution provides a good opportunity for the application of NOMA. By selecting any

beam as a NOMA user, since $R^N > 0$, the overall rate increases significantly. However, when users are distributed along two or four straight lines, the performance of the LDMA-based scheme is no longer extremely low, though it still falls short of the beam efficiency of the proposed LDMA-NOMA hybrid scheme. Specifically, for example, in subfigure (b) with $K = 20$ and in subfigure (c) with $K = 40$, the beam efficiency of the LDMA-based scheme is only slightly lower than that of the LDMA-NOMA hybrid scheme. This is because the resolution between U_0 and other users is good, allowing the LDMA-based scheme to be effectively applied. However, it can still be observed from the figure that if NOMA users are selected appropriately, the beam efficiency can still be significantly improved. This is because there are still users whose resolution between other users are not good. The LDMA-NOMA hybrid scheme accurately identifies such user pairs and utilizes the fact of their poor resolution to maximize beam efficiency. In addition, it can be observed that as the number of users increases, the beam efficiency decreases. The reason is evident, serving more users with the same resources leads to increased interference among users, resulting in a decline in system performance. However, even in scenarios with a large number of users, the proposed scheme in this paper still provides a significant advantage.

Fig. 7 presents the impact of the number of transmitting antennas on the performance of the two schemes. All users are uniformly distributed along a single straight line, identical to the scenario in Fig. 6(a). The SNR is set to $\rho = 40$ dB. The number of antennas $M = 32$ is fixed, while N varies from 32 to 512. It can be observed from the figure that as N increases, the beam efficiency of both schemes also increases until it reaches the upper bound, beyond which it no longer grows. The reason can be explained as follows. When N is not large, as N increases, the resolution between users gradually improves, leading to an increase in the performance. However, when N is larger than a certain value, the resolution tends to be a non-zero constant, and further increasing N does not lead to performance improvement. This also has been explained in previous works in the literature [22], [23]. Additionally, it can be observed from the figure that as N increases, the performance difference between the two schemes becomes smaller until they are almost identical. This indicates that as long as the number of transmitting antennas is sufficiently large, the LDMA-based scheme can also achieve a good performance. However, when the number of antennas is not large enough, the LDMA-NOMA hybrid scheme is still superior. Furthermore, it can be noticed from the figure that more users imply poorer performance, which is consistent with the finding in Fig. 6.

Fig. 8 presents the beam efficiency under conditions of limited beam resources, applying the grouping algorithm proposed in this paper. For comparison, the results of random grouping are also shown in the figure. The user distribution and other physical parameters are the same as those in Fig. 6. From the figure, it can be seen that after grouping using the algorithm proposed in this paper, the beam efficiency is significantly improved compared to random grouping. This indicates that the proposed algorithm effectively utilizes the

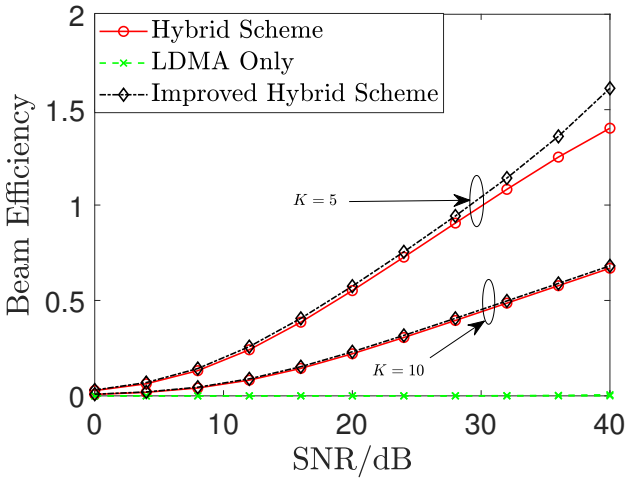

(a) The users are distributed linearly. $\theta = \frac{\pi}{6}, \phi = \frac{\pi}{6}$.

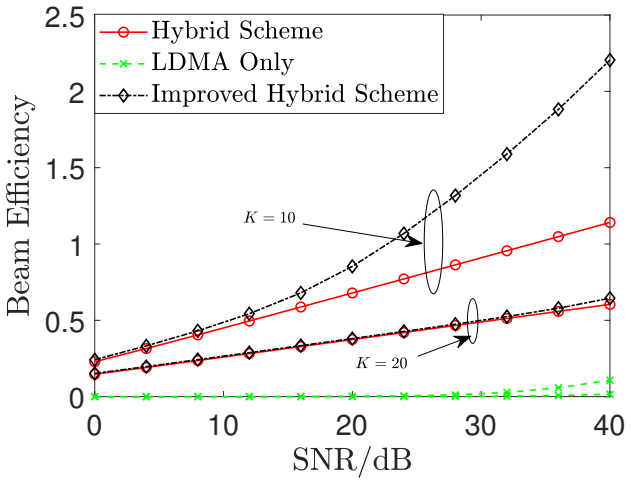

(b) The users are distributed along two straight lines. $\theta_1 = -\frac{\pi}{6}, \theta_2 = \frac{\pi}{6}, \phi = \frac{\pi}{6}$.

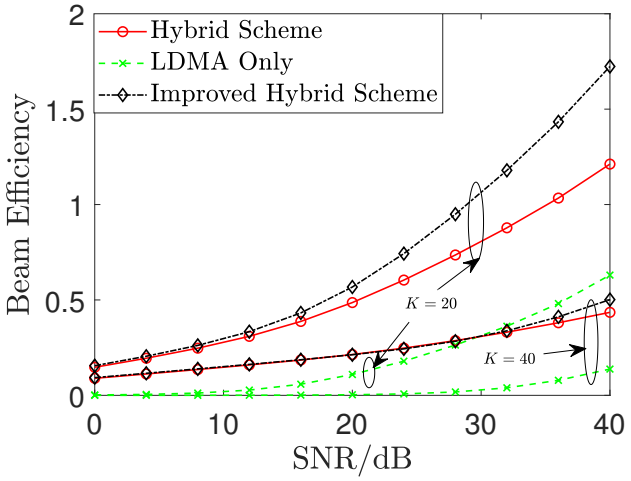

(c) The users are distributed along four straight lines. $\theta_1 = -\frac{\pi}{3}, \theta_2 = -\frac{\pi}{9}, \theta_3 = \frac{\pi}{9}, \theta_4 = \frac{\pi}{3}, \phi = \frac{\pi}{6}$.

Fig. 6. Comparison of the proposed scheme and LDMA-based scheme in terms of beam efficiency.

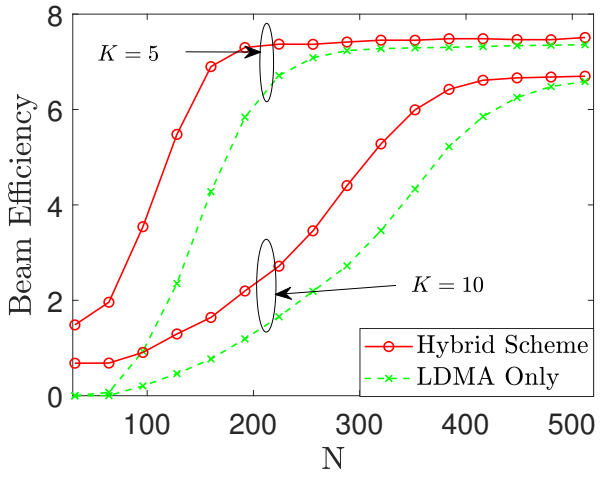

Fig. 7. The impact of the number of antennas on the beam efficiency of the two schemes when user positions are fixed.

resolution between users to enhance system performance. Particularly, in subfigures (a) and (b), it can be observed that increasing the SNR has little impact on the performance improvement of random grouping. This is because incorrect grouping may apply NOMA to two users with good resolution, while applying LDMA to two users with poor resolution, thus failing to effectively utilize the advantages of both multiple access schemes. This emphasizes the importance of accurate grouping of users based on their resolution. Additionally, it can be observed from the figure that as the beam resources K_L increase, the beam efficiency decreases. This is because although increasing the beam resources improves the overall information rate, the amount of increase cannot match the number of consumed beam resources, resulting in a decrease in the beam efficiency. This further highlights the significant improvement in the beam efficiency realized by the proposed hybrid LDMA-NOMA scheme in our work.

To study the impact of the number of available beams on the beam efficiency, the results for different K_L are presented in Fig. 9. Two cases of different user distribution model, distributed linearly in a line and distributed uniformly in two lines are considered. The parameters of the communication system are the same as in Fig. 6. It can be observed from the figure that the beam efficiency is inversely correlated with K_L. The reason is that the improvement of rate brought by the increasing of K_L cannot match the number of utilized beam resources, which is also discussed in Fig. 8. When $K_L \geq 20$, the utilization of beam resources has been saturated, the beam efficiency cannot be improved by just increasing the transmission power. In addition, it can be seen from the figure that the case of uniform distribution performs better than the case of linear distribution. This is because the resolution of users distributed in a line is much worse, and leads to performance loss. This also demonstrates the significance in the proposed hybrid LDMA-NOMA scheme.

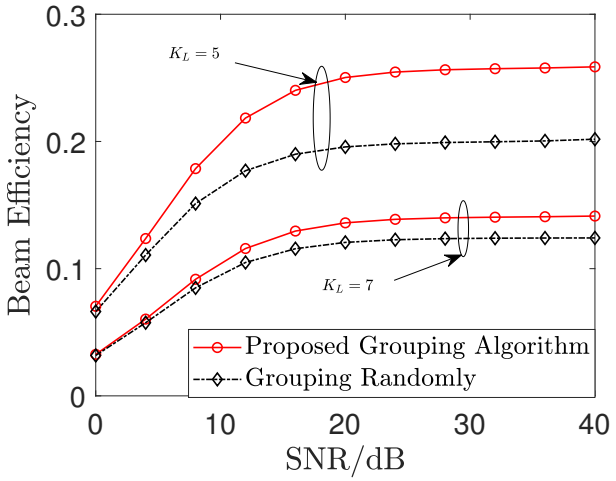

(a) The users are distributed linearly. $\theta = \frac{\pi}{6}, \phi = \frac{\pi}{6}$, $K = 10$.

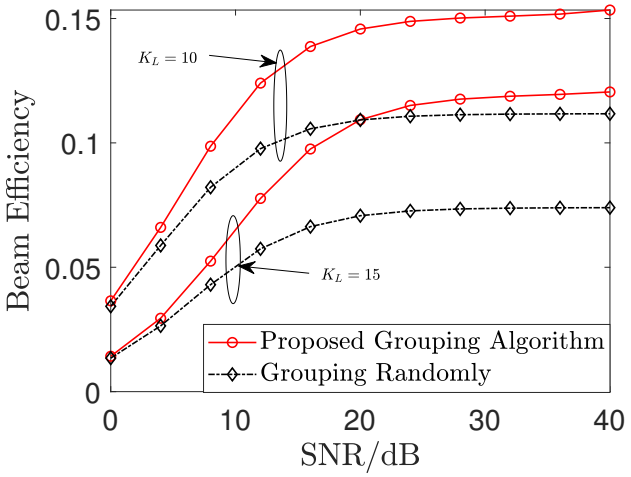

(b) The users are distributed along two straight lines. $\theta_1 = -\frac{\pi}{6}, \theta_2 = \frac{\pi}{6}, \phi = \frac{\pi}{6}$, $K = 20$.

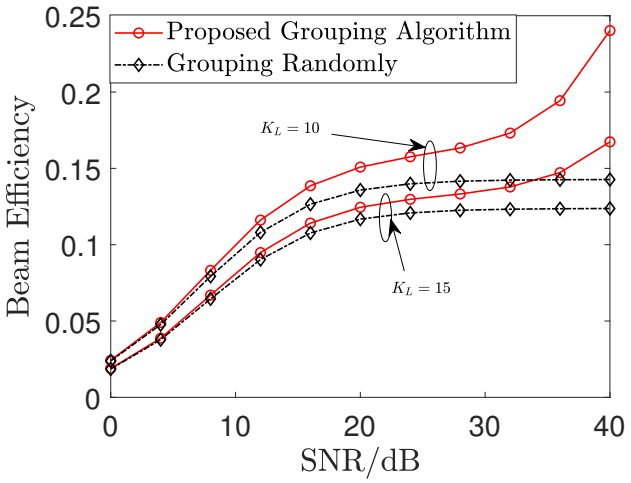

(c) The users are distributed along four straight lines. $\theta_1 = -\frac{\pi}{3}, \theta_2 = -\frac{\pi}{9}, \theta_3 = \frac{\pi}{9}, \theta_4 = \frac{\pi}{3}, \phi = \frac{\pi}{6}$, $K = 30$.

Fig. 8. Performance comparison of the proposed scheme and arbitrarily grouping scheme with limited beam resources.

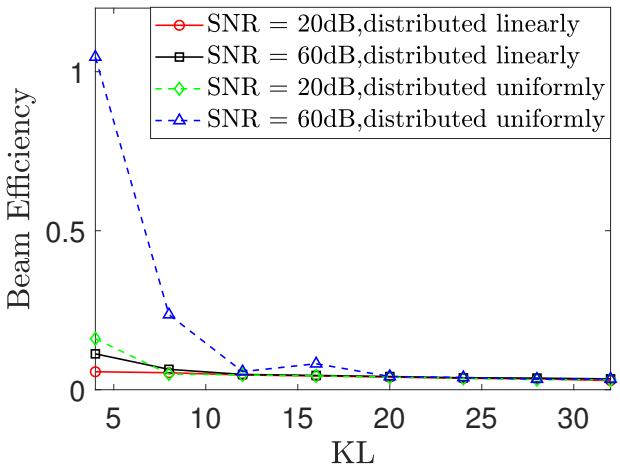

Fig. 9. The impact of the number of available beams on the beam efficiency.

VII. Conclusion

In this paper, we proposed a novel LDMA-NOMA hybrid scheme for near-field communication beamforming, which uniquely combines the advantages of location-division multiple access (LDMA) and non-orthogonal multiple access (NOMA). The key innovation of proposed scheme lies in its ability to dynamically allocate beam resources based on user resolution information, optimizing beam efficiency. The performance of the proposed scheme was also analyzed. Simulation results were provided to demonstrate the benefits of the proposed scheme, drawing a performance comparison against different benchmark schemes, highlighting its potential to significantly enhance beamforming performance in near-field communication scenarios.

Appendix A
Proof of Corollary 2

When $\rho \to +\infty$, $g(\mathbf{F}_A, \mathbf{b}_0)$ can be known as

$$g(\mathbf{F}_A, \mathbf{b}_0) \to \frac{[(\mathbf{F}_{A,0}^H \mathbf{F}_{A,0})^{-1}]_{1,1}}{\rho \alpha_0^2 l_0} \times \prod_{k=1}^{K} \frac{[(\mathbf{F}_{A,0}^H \mathbf{F}_{A,0})^{-1}]_{k+1,k+1}}{[(\mathbf{F}_A^H \mathbf{F}_A)^{-1}]_{k,k}}. \tag{56}$$

Then $f(\Delta_{0,1})$ can be known as

$$\begin{aligned} f(\Delta_{0,1}) &\to \Delta_{0,1} - \frac{\sum_{j=1}^{K} |\mathbf{h}_0^H \mathbf{F}_A \mathbf{f}_{D,j}|^2 l_j}{\alpha_0^2 l_0} \left(\frac{1}{g(\mathbf{F}_A, \mathbf{b}_0)} - 1 \right) \\ &= \Delta_{0,1} - C_1 \rho + C_2, \end{aligned} \tag{57}$$

where

$$\begin{aligned} C_1 &= \sum_{j=1}^{K} |\mathbf{h}_0^H \mathbf{F}_A \mathbf{f}_{D,j}|^2 l_j \prod_{k=1}^{K} \frac{[(\mathbf{F}_{A,0}^H \mathbf{F}_{A,0})^{-1}]_{k+1,k+1}}{[(\mathbf{F}_A^H \mathbf{F}_A)^{-1}]_{k,k}}, \\ C_2 &= \frac{\sum_{j=1}^{K} |\mathbf{h}_0^H \mathbf{F}_A \mathbf{f}_{D,j}|^2 l_j}{\alpha_0^2 l_0}. \end{aligned} \tag{58}$$

The first part of the Corollary is proved.

When $\rho \to 0$, $g(\mathbf{F}_A, \mathbf{b}_0)$ can be known as

$$g(\mathbf{F}_A, \mathbf{b}_0) \to \left(1 + \frac{\rho \alpha_0^2 l_0}{[(\mathbf{F}_{A,0}^H \mathbf{F}_{A,0})^{-1}]_{1,1}} \right)^{-1}. \tag{59}$$

Then $f(\Delta_{0,1})$ can be known as

$$\begin{aligned} f(\Delta_{0,1}) &\to \Delta_{0,1} - \frac{1}{\rho \alpha_0^2 l_0} \left(\frac{1}{g(\mathbf{F}_A, \mathbf{b}_0)} - 1 \right) \\ &= \Delta_{0,1} - \frac{1}{[(\mathbf{F}_{A,0}^H \mathbf{F}_{A,0})^{-1}]_{1,1}} \\ &= \Delta_{0,1} - (1 - \mathbf{b}_0^H \mathbf{F}_A (\mathbf{F}_A^H \mathbf{F}_A)^{-1} \mathbf{F}_A^H \mathbf{b}_0). \end{aligned} \tag{60}$$

The second part of the Corollary is proved.

Appendix B
Proof of Corollary 3

We prove the corollary based on different cases of I_l for the l-th user:

- When $I_l \approx 1$. This requires users to meet the following conditions:
  - $\sum_{j=1}^{K_L} \lambda_j^2 \Delta_{l,j}^{N,L} \approx 0$, i.e., $\lambda_j \approx 0$ with any $1 \leq j \leq K_L$. This condition occurs when the resolution between LDMA users is poor.
  - $\sum_{i=1, i \neq l, i \notin \mathbf{h}(l)}^{K_N} \Delta_{l,g^{-1}(i)}^{N,L} l_i^N \approx 0$, i.e., there is no interference between NOMA users assigned to the same beam. This can almost only occur after the final stage of SIC is completed, so at most one user per beam can meet this condition.

  If both conditions are met, then $\gamma_l^N = C_N \rho$, where C_N is a constant that independent of ρ.
- When $I_1 > 1$, i.e., either of the above conditions is not met, then γ_l^N can be approximated as follows:

$$\gamma_l^L \approx \frac{\Delta_{l,g^{-1}(l)}^{N,L} l_l^N}{\sum_{j=1}^{K_L} |\mathbf{b}_l^{NH} \mathbf{F}_A \mathbf{f}_{D,j}|^2 l_j^L + \sum_{i=1, i \neq l, i \notin \mathbf{h}(l)}^{K_N} \Delta_{l,g^{-1}(i)}^{N,L} l_i^N}, \tag{61}$$

  which is independent of ρ.

Denote $0 \leq K_{N,0} \leq K_{Beam}$ as the number of users that satisfy both conditions, where K_{Beam} is the number of beams that carry any NOMA user. Then R can be approximated as follows:

$$\begin{aligned} R &= K_L \log(1 + C_L \rho) + K_{N,0} \log(1 + C_N \rho) \\ &\approx (K_L + K_{N,0}) \log(\rho), \end{aligned} \tag{62}$$

where C_L, is constant that independent of ρ. Based on the range of K_N, the result of the corollary can be derived.

References

[1] C.-X. Wang, X. You, X. Gao, X. Zhu, Z. Li, C. Zhang, H. Wang, Y. Huang, Y. Chen, H. Haas, J. S. Thompson, E. G. Larsson, M. D. Renzo, W. Tong, P. Zhu, X. Shen, H. V. Poor, and L. Hanzo, "On the road to 6g: Visions, requirements, key technologies, and testbeds," *IEEE Communications Surveys & Tutorials*, vol. 25, no. 2, pp. 905–974, 2023.

[2] Huawei. (2022) 6g: The next horizon white paper. [Online]. Available: https://www.huawei.com/en/huaweitech/future-technologies/6g-white-paper

[3] L. Lu, G. Y. Li, A. L. Swindlehurst, A. Ashikhmin, and R. Zhang, "An overview of massive MIMO: Benefits and challenges," *IEEE Journal of Selected Topics in Signal Processing*, vol. 8, no. 5, pp. 742–758, Apr. 2014.

[4] F. A. Pereira de Figueiredo, "An overview of massive MIMO for 5G and 6G," *IEEE Latin America Transactions*, vol. 20, no. 6, pp. 931–940, Apr. 2022.

[5] L. Sanguinetti, E. Björnson, and J. Hoydis, "Toward massive MIMO 2.0: Understanding spatial correlation, interference suppression, and pilot contamination," *IEEE Transactions on Communications*, vol. 68, no. 1, pp. 232–257, Oct. 2020.

[6] M. Cui and L. Dai, "Near-field wideband beamforming for extremely large antenna arrays," *IEEE Transactions on Wireless Communications*, pp. 1–1, 2024.

[7] W. H. Southwell, "Validity of the fresnel approximation in the near field," *J. Opt. Soc. Am.*, vol. 71, no. 1, pp. 7–14, Jan. 1981.

[8] K. T. Selvan and R. Janaswamy, "Fraunhofer and fresnel distances: Unified derivation for aperture antennas," *IEEE Antennas and Propagation Magazine*, vol. 59, no. 4, pp. 12–15, Jun. 2017.

[9] Y. Liu, Z. Wang, J. Xu, C. Ouyang, X. Mu, and R. Schober, "Near-field communications: A tutorial review," *IEEE Open Journal of the Communications Society*, Aug. 2023.

[10] Y. Han, S. Jin, C.-K. Wen, and X. Ma, "Channel estimation for extremely large-scale massive MIMO systems," *IEEE Wireless Communications Letters*, vol. 9, no. 5, pp. 633–637, 2020.

[11] M. Cui and L. Dai, "Channel estimation for extremely large-scale MIMO: Far-field or near-field?" *IEEE Transactions on Communications*, vol. 70, no. 4, pp. 2663–2677, 2022.

[12] X. Zhang, Z. Wang, H. Zhang, and L. Yang, "Near-field channel estimation for extremely large-scale array communications: A model-based deep learning approach," *IEEE Communications Letters*, vol. 27, no. 4, pp. 1155–1159, 2023.

[13] X. Zhang, H. Zhang, J. Zhang, C. Li, Y. Huang, and L. Yang, "Codebook design for extremely large-scale MIMO systems: Near-field and far-field," *IEEE Transactions on Communications*, vol. 72, no. 2, pp. 1191–1206, 2024.

[14] L. Dai, J. Tan, Z. Chen, and H. V. Poor, "Delay-phase precoding for wideband thz massive MIMO," *IEEE Transactions on Wireless Communications*, vol. 21, no. 9, pp. 7271–7286, 2022.

[15] M. Cui, L. Dai, Z. Wang, S. Zhou, and N. Ge, "Near-field rainbow: Wideband beam training for XL-MIMO," *IEEE Transactions on Wireless Communications*, vol. 22, no. 6, pp. 3899–3912, 2023.

[16] N. Decarli and D. Dardari, "Communication modes with large intelligent surfaces in the near field," *IEEE Access*, vol. 9, pp. 165 648–165 666, 2021.

[17] Z. Wu, M. Cui, Z. Zhang, and L. Dai, "Distance-aware precoding for near-field capacity improvement in XL-MIMO," in *2022 IEEE 95th Vehicular Technology Conference: (VTC2022-Spring)*, 2022, pp. 1–5.

[18] L. Yan, Y. Chen, C. Han, and J. Yuan, "Joint inter-path and intra-path multiplexing for terahertz widely-spaced multi-subarray hybrid beamforming systems," *IEEE Transactions on Communications*, vol. 70, no. 2, pp. 1391–1406, 2022.

[19] S. Guo and K. Qu, "Beamspace modulation for near field capacity improvement in XL-MIMO communications," *IEEE Wireless Communications Letters*, vol. 12, no. 8, pp. 1434–1438, 2023.

[20] N. J. Myers and R. W. Heath, "Infocus: A spatial coding technique to mitigate misfocus in near-field LoS beamforming," *IEEE Transactions on Wireless Communications*, vol. 21, no. 4, pp. 2193–2209, 2022.

[21] Z. Wu and L. Dai, "Multiple access for near-field communications: SDMA or LDMA?" *IEEE Journal on Selected Areas in Communications*, vol. 41, no. 6, pp. 1918–1935, Jun. 2023.

[22] Z. Ding, "Resolution of near-field beamforming and its impact on NOMA," *IEEE Wireless Communications Letters*, pp. 1–1, Nov. 2023.

[23] C. Rao, Z. Ding, O. A. Dobre, and X. Dai, "A general analytical framework for the resolution of near-field beamforming," *IEEE Communications Letters*, vol. 28, no. 5, pp. 1171–1175, 2024.

[24] M. Cui, Z. Wu, Y. Lu, X. Wei, and L. Dai, "Near-field MIMO communications for 6G: Fundamentals, challenges, potentials, and future directions," *IEEE Communications Magazine*, vol. 61, no. 1, pp. 40–46, Sep. 2023.

[25] Z. Ding, "NOMA beamforming in SDMA networks: Riding on existing beams or forming new ones?" *IEEE Communications Letters*, vol. 26, no. 4, pp. 868–871, Apr 2022.

[26] H. Abdi and L. J. Williams, "Principal component analysis," *Wiley interdisciplinary reviews: computational statistics*, vol. 2, no. 4, pp. 433–459, 2010.

Chenguang Rao received the B.S. degree from the University of Science and Technology of China in 2019, where he is currently pursuing the Ph.D degree with the Department of Electronic Engineering and Information Science. His current research interests include random matrix, multiple access systems and near field communications.

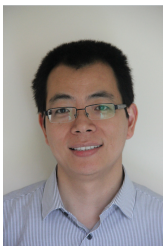

ZhiguoDing (S'03-M'05-F'20) received his B.Eng in Electrical Engineering from the Beijing University of Posts and Telecommunications in 2000, and the Ph.D degree in Electrical Engineering from Imperial College London in 2005. He is currently a Professor at Khalifa University, and an Academic Visitor at Princeton University. Previously, he had worked at Queen's University Belfast, Imperial College, Newcastle University, and Lancaster University. Dr Ding' research interests are 6G networks, communications and signal processing. His h-index is over 100 and his work receives 60,000+ Google citations. He is serving as an Area Editor for the IEEE TWC and TCOM, an Editor for IEEE TVT, and OJ-SP, and was an Area Editor for IEEE OJCOMS, an Editor for IEEE TCOM, TWC, COMST, WCL, CL and WCMC. He received the best paper award of IET ICWMC-2009 and IEEE WCSP-2014, the EU Marie Curie Fellowship 2012-2014, the Top IEEE TVT Editor 2017, IEEE Heinrich Hertz Award 2018, IEEE Jack Neubauer Memorial Award 2018, IEEE Best Signal Processing Letter Award 2018, Alexander von Humboldt Foundation Friedrich Wilhelm Bessel Research Award 2020, IEEE SPCC Technical Recognition Award 2021, IEEE VTS Best Magazine Paper Award 2023, and the Best Paper Award in IEEE GLOBCOM 2024. He is a Web of Science Highly Cited Researcher in two disciplines (2019-2024), an IEEE ComSoc Distinguished Lecturer, and a Fellow of the IEEE.

Kanapathippillai Cumanan (M'10, SM'19) received the BSc degree with first class honors in electrical and electronic engineering from the University of Peradeniya, Sri Lanka in 2006 and subsequently obtained his PhD degree in signal processing for wireless communications from Loughborough University, Loughborough, UK, in 2009. He is currently a Professor of Wireless Communications at the School of Physics, Engineering and Technology, University of York, UK. Prior to this he served as an Assistant Lecturer at the Department of Electrical and Electronic Engineering, University of Peradeniya, Sri Lanka from January 2006 to August 2006. Between January 2010 and March 2012, he held a Research Associate position at Loughborough University, UK, followed by a similar role at Newcastle University, Newcastle upon Tyne, UK from March 2012 to November 2014. He joined as lecturer at University of York, UK in November 2014. In 2011, he was also an Academic Visitor at the Department of Electrical and Computer Engineering, National University of Singapore. His research interests include non-orthogonal multiple access (NOMA), cell-free massive MIMO, physical layer security, cognitive radio networks, convex optimization techniques and resource allocation techniques. He has published more than 100 journal articles and conference papers which have collectively received more than 4500 Google scholar citations. Dr. Cumanan was the recipient of an overseas research student award scheme (ORSAS) from Cardiff University, Wales, UK, where he was a research student between September 2006 and July 2007.

Xuchu Dai received the B.Eng. degree in electrical engineering from Air force Engineering University, Xian, China, in 1984, and the M.Eng. and Ph.D. degrees in communication and information systems from the University of Science and Technology of China, Hefei, China, in 1991 and 1998, respectively. He was with the Hong Kong University of Science and Technology as a Post-Doctoral Researcher from 2000 to 2002. He is currently a Professor with the Department of Electronic Engineering and Information Science, University of Science and Technology of China. His current research interests include wireless communication systems, blind adaptive signal processing, and signal detection.